Chapter 2

Chlorophyll Biodegradation

Nina Djapic

Additional information is available at the end of the chapter

http://dx.doi.org/10.5772/56155

1. Introduction

One of the most important biochemical processes is photosynthesis and life depends on the conversion of the solar energy into a chemical one. It occurs in photoautotrophic organisms. The chlorophyll *a* is supported by chlorophyll *b*, carotenes and xanthophylls in the light capture. The chlorophyll *a* and accessory pigments are found in cell organelles called chloroplasts. The conversion of light energy into the chemical one can be described thermodynamically. The entropy of photosynthesis yields the energy of 27.32 kJ mol^{-1} and is a source of energy for the plants. The atmospheric oxygen is a product of the oxygenic photosynthesis, the product of the first phase process known as light – dependant reactions. In those reactions, the chlorophylls, in the so called reaction centre, function as an absorbent of a photon initiating the electron transport chain, with the loss of an electron. During the electron flow the energy is produced and the reduced form of the nicotinamide adenine dinucleotide phosphate (NADPH) and the adenosine triphosphate (ATP) are formed. The chlorophyll molecule regains the electron from water. The other phase of photosynthesis is called the light – independent reactions or the Calvin cycle. In those reactions the enzyme ribulose-1, 5-bisphosphate carboxylase/oxygenase (RuBisCO) captures the CO_2 from the atmosphere and during the Calvin cycle glucose is formed. The light-absorbing green pigments, the chlorophylls, are biodegraded under various conditions: with the leaf senescence in autumn, under stress conditions, such as, drought, flooding, chilling, mechanical wounding, etc., under the exposure to the ethylene and after the treatment of plants with herbicides. In autumn deciduous trees shed tones of leaves. The green leaves change the colour due to the chlorophyll biodegradation. The peculiarity of the chlorophyll biodegradation in autumnal leaves will be described.

2. Chlorophyll biodegradation

The chlorophyll *a* and chlorophyll *b* biodegradation pathways consist of a great number of steps and up to now only the steps where the chlorophylls' biodegradation products have a chromophore that can absorb the ultra-violet (UV)/visible light are known. Each step can be considered separately. In the cell, every step is coordinated, highly regulated and most steps are enzymatically catalyzed. The first group of reactions includes the loss of magnesium, the loss of phytol and the modifications on the periphery of the chlorophyll nucleus in which the aromatic tetrapyrrole macrocycle remains intact [1]. The starting investigations on chlorophylls and chlorophylls' biodegradation products were done by Richard Willstaetter and Arthur Stoll who have discovered the nature of the chlorophylls [2]. Ivan Parfen'ievitch Borodin was the first who obtained crystalline chlorophyll [2]. Finally, Mikhail Semenovitch Tswett, after the formulation of the chromatography method, proved that the chlorophyll was a mixture of two green pigments "chlorophyllins alfa and beta" and that Ivan Parfen'ievitch Borodin's pigment is different from natural chlorophylls [3, 4, 5, 6]. Richard Willstaetter and Arthur Stoll showed that green leaves contain an enzyme chlorophyllase which hydrolyses the phytyl ester of the chlorophylls' propionate group to yield chlorophyllide *a* [2, 7, 8]. In the presence of alcohol, the crystalline substance formed by transesterification, is methyl chlorophyllide [9]. Richard Willstaetter and Arthur Stoll determined the basic structure of chlorophyll *a* and *b* and showed that Ivan Parfen'ievitch Borodin's crystalline pigments were chlorophyllide *a* and *b* formed from natural chlorophylls by the hydrolysis by the enzyme chlorophyllase [10].

The interconversion of chlorophyll *b* to chlorophyll *a* and vice versa occurs in oxygenic photosynthetic organisms [11]. The suggested chlorophyll cycle is depicted in Figure 1. The cycle starts with the reduction of chlorophyll *b* by chlorophyll *b* reductase, an NADPH dependant enzyme, to form 7^1–hydroxyl chlorophyll *a*. The 7^1–hydroxyl chlorophyll *a* is a stable intermediate and it was isolated from higher plants. The next reduction step is catalyzed by ferredoxin dependant 7^1–hydroxyl chlorophyll *a* reductase to form chlorophyll *a*. It is also suggested that chlorophyll *a* interconverts to chlorophyll *b* by an oxygen dependant enzyme chlorophyll *a* oxygenase. The enzyme oxidizes chlorophyll *a* to 7^1–hydroxyl chlorophyll *a* which is further oxidized to chlorophyll *b* by 7^1–hydroxyl chlorophyll *a* dehydrogenase.

The bioconversion of chlorophyll *b* to chlorophyll *a* undergoes through a 7^1–hydroxyl intermediate. The chlorophyll interconversion cycle can be expanded to the following catabolic steps toward the chlorophyllide *a* (Figure 1). The chlorophyll *a* is enzymatically hydrolysed to chlorophyllide *a*. The chlorophyll *b* is enzymatically hydrolysed to chlorophyllide *b* and undergoes through the formation of 7^1–hydroxyl chlorophyllide *a* which is enzymatically reduced to the chlorophyllide *a* [12].

Richard Willstaetter observed that the ash from the crude chlorophylls is rich in magnesia [2]. The magnesium is cleaved from the chlorophylls by a treatment with mild acids. The magnesium coordination bond is stable against alkali [9]. On the other hand, treatment with hydroxide saponifies the chlorophylls' phytol side chain yielding chlorophyllides.

http://dx.doi.org/10.5772/56155

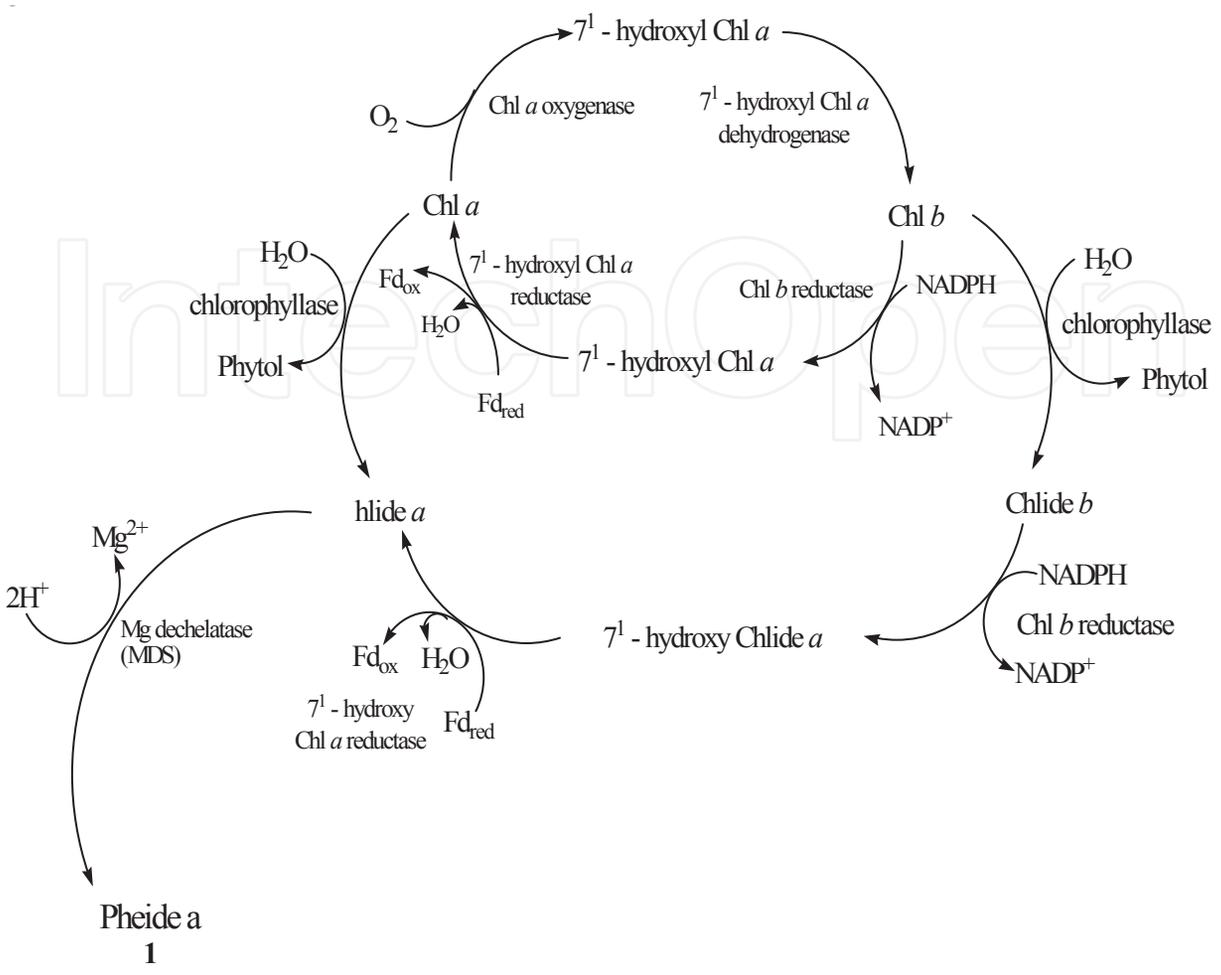

Figure 1. The chlorophyll cycle

The chlorophyll biodegradation continues with dechelating the chlorophyllide *a* molecule. The enzyme involved in demetallation is Mg–dechelatase. A catalytic cofactor called Mg–dechelating substance (MDS) is associated with the activity of Mg–dechelatase [13]. When the magnesium is expelled from the core of chlorophyllide *a*, the remaining structure is called pheophorbide *a* (1) (Figure 1).

The next group of reactions involves the cleavage of the macrocyclic aromatic ring system yielding open chain tetrapyrrolic compound, the *seco*–phytoporhyrins, in which side chains can be further modified. In further chlorophyll biodegradation, pheophorbide *a* (1) methene bridge at the C4–C5 position is oxidized by the pheophorbide *a* oxygenase (P*a*O) to yield the 4,5-dioxo-*seco*-pheophorbide *a* chlorophyll biodegradation product (2). The P*a*O is an iron–dependant monooxygenase. The electrons required for the redox cycle are supplied from the reduced ferredoxin (Figure 2).

The proposed mechanism is based on the single oxygen attachment to the double bond at the C4=C5 position forming regioselective intermediate by the cleavage of the oxirane ring.

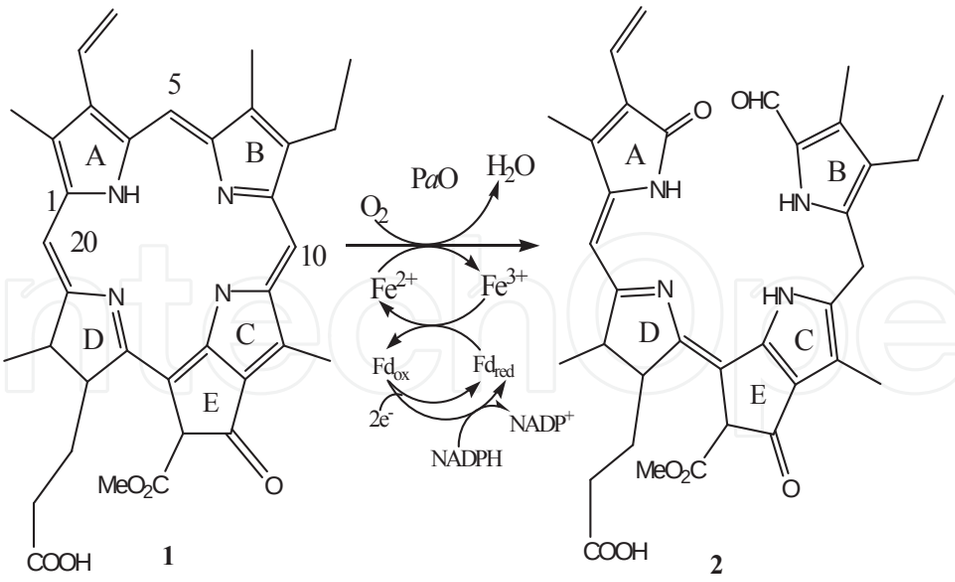

Figure 2. The proposed mechanism of the pheophorbide *a* (1) oxidation, by the PaO to the 4,5-dioxo- *seco*-pheophorbide *a* (2).

Subsequently, the oxiran ring is opened hydrolytically. The retro–aldol reaction proceeds and the rearrangement of protons form the 4,5-dioxo-*seco*-pheophorbide *a* (2) (Figure 2).

The amount of accumulated chlorophyll biodegradation products within the same plant species varies. The quantity of the chlorophyll biodegradation products in senescent leaves most probably depends on the time of the collection, seasonal climate, developmental stage of the plant, enzymes, etc. One of the reasons for the chlorophyll biodegradation in biological systems is due to the tendency of the organism to decrease the level of photodynamically active chlorophyll before the programmed cell death [14].

3. Chlorophyll biodegradation in Hamamelidaceae and Vitaceae autumnal leaves

The autonomous induction of leaf senescence occurs in autumn. The major consequence of leaf senescence is chlorophyll biodegradation. The crude methanol extracts of Hamamelidaceae and Vitaceae autumnal leaves' plant species were analyzed on the reversed phase (RP): RP–C_8 and RP–C_4 analytical columns by liquid chromatography–mass spectrometry (LC–MS) and their structure was determined by mass and nuclear magnetic resonance (NMR) spectra [15, 16, 17]. The results obtained gave insight in the chlorophyll biodegradation in plant species of Hamamelidaceae and Vitaceae autumnal leaves (Figure 3). The chlorophyll biodegradation pathway continues from the 4, 5-dioxo-*seco*-pheophorbide *a* (2) to the formation of the hydroxylated ethyl side chain chlorophyll biodegradation product (3). The enzyme catalyzing the hydroxylation of the ethyl side chain is still unknown.

http://dx.doi.org/10.5772/56155

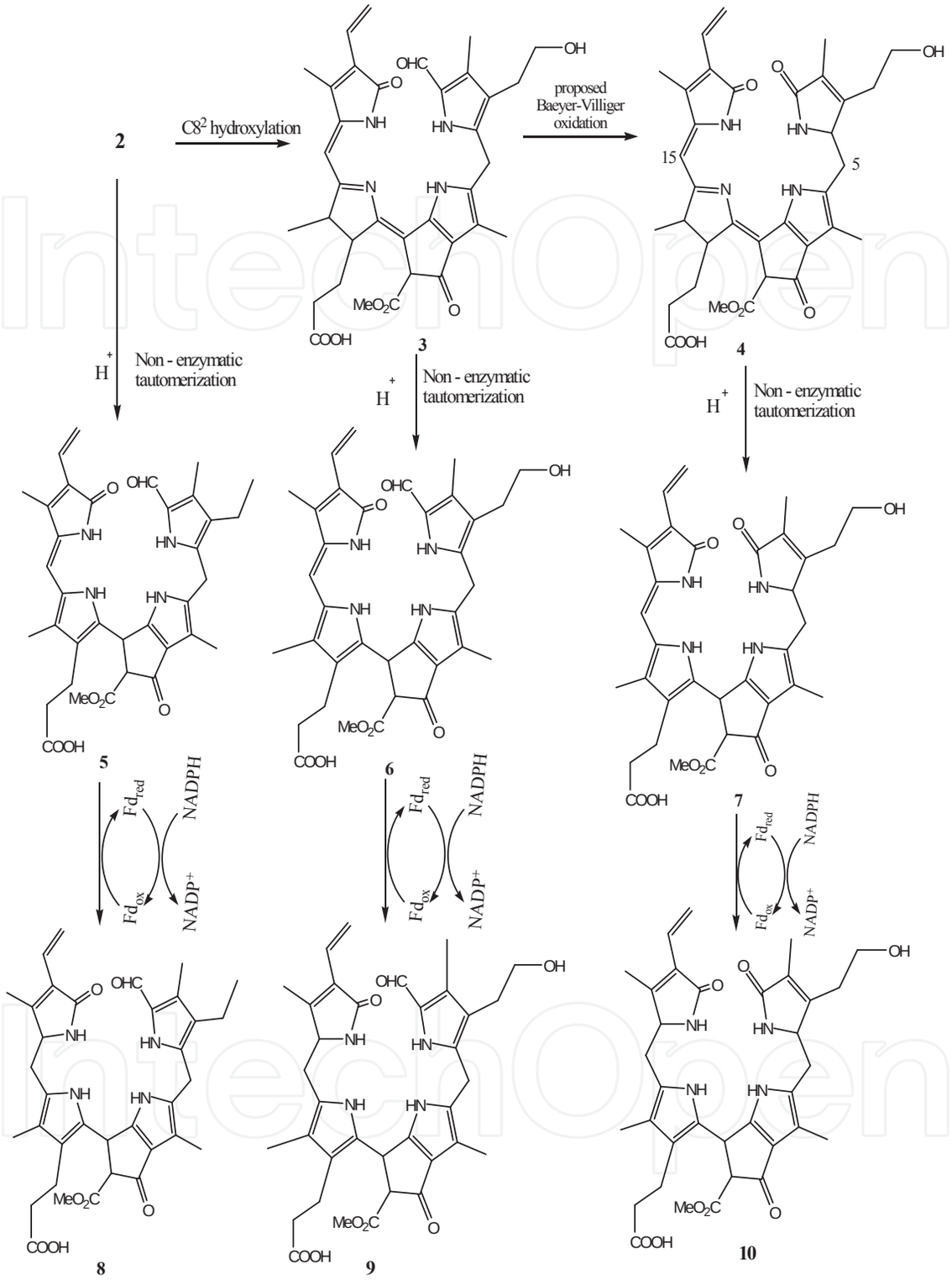

Figure 3. The chlorophyll biodegradation pathway in Hamamelidaceae and Vitaceae autumnal leaves. The ethyl side chain of the 4, 5-dioxo-*seco*-pheophorbide *a* (2) is enzymatically hydroxylated to the compound 3 and after the proposed Baeyer-Villiger oxidation the urobilinogenic chlorophyll biodegradation product (4) is formed. All chlorophyll biodegradaton products under acid conditions form the thermodynamically more stable compounds (5, 6, 7). The reduction of the chlorophyll biodegradation compounds 5, 6 and 7 proceeds via the reduction of the "western" methene bridge forming the chlorophyll biodegradation products 8, 9 and 10.

The urobilinogenic chlorophyll biodegradaton products isolated from autumnal leaves of *Parrotia persica* and *Hamamelis virginiana*, Hamamelidaceae significantly differ from other isolated chlorophyll biodegradation products in one functional group [15, 16]. The aldehyde group at C5 position is absent and chlorophyll biodegradation product's structure refers to the urobilinogen. The aldehyde group at the C5 (3) position might be oxidized by Baeyer–Villiger monooxygenase. The carbon numeration differs from all previously isolated chlorophyll biodegradation products and is as in urobilinogen (Figure 3) [15, 16].

The proposed oxidation step is by the Baeyer–Villiger monooxygenase, from the $C8^2$-hydroxylated chlorophyll biodegradation product (3) to the urobilinogenic chlorophyll biodegradation product (4). The oxidation results in the formation of an additional chiral centre at the position C4. The absolute configuration of all chiral centres is unknown. It is proposed that this enzyme can convert the chlorophyll biodegradation product's aldehyde group into the corresponding dehydro pyrrolidin–2–one of the urobilinogenic chlorophyll biodegradation product mediated by the hydroperoxide intermediate. The nucleophilic addition of the hydroperoxide to the C5 oxo group affords peroxide intermediate. After the rearrangement, the insertion of the oxygen is made. After the ester hydrolysis, the alcohol is formed [17, 18, 19]. After the acidic catalyzed tautomerization, the urobilinogenic chlorophyll biodegradation product is formed. Another conceivable mechanism that can explain the formation of the urobilinogenic chlorophyll biodegradation product is by the oxidative decarboxylation of an acid intermediate generated by the oxidation of the aldehyde group.

The chlorophyll biodegradation products (2, 3, 4) form the thermodynamically more stable compounds (5, 6, 7) after the acidic catalyzed tautomerization, [20]. The reduction of the compounds 5, 6 and 7 proceed via the reduction of the "western" methene bridge. It is catalyzed by a reductase. The reductase is a ferredoxin dependant enzyme with no requirements of cofactors such as flavin or metals. After the reduction of the chlorophyll biodegradation products 5, 6, 7 the chlorophyll biodegradation products 8, 9 and 10 are formed.

Further chlorophyll biodegradation products were, up to now, not detected. The further chlorophyll biodegradation products lose the chromophore that can absorb the UV light, they become colourless, and were not identified up to now.

4. Chlorophyll biodegradation in Solanaceae autumnal leaves

In autumnal leaveas of the Solanaceae family: tobacco (*Nicotiana tabacum*), potatoe (*Solanum tuberosum*), *Atropa belladonna*, etc. chlorophyll biodegradation products are present. In Solanaceae plant species the 4, 5-dioxo-*seco*-pheophorbide *a* (2) precedes, in further chlorophyll biodegradation, the hydroxylation at the $C8^2$ position and then the glycosylation at the $C8^2$ position (11) [21]. The glycosyl bond is most probably introduced by glycosyltransferase. The Solanaceae chlorophyll biodegradation product (11) form a thermodynamically stable aromatic ring D under the acidic conditions (12) (Figure 4). The reduction of the thermodynamically more stable compound (12) proceeds via the reduction of the "western" methene

http://dx.doi.org/10.5772/56155

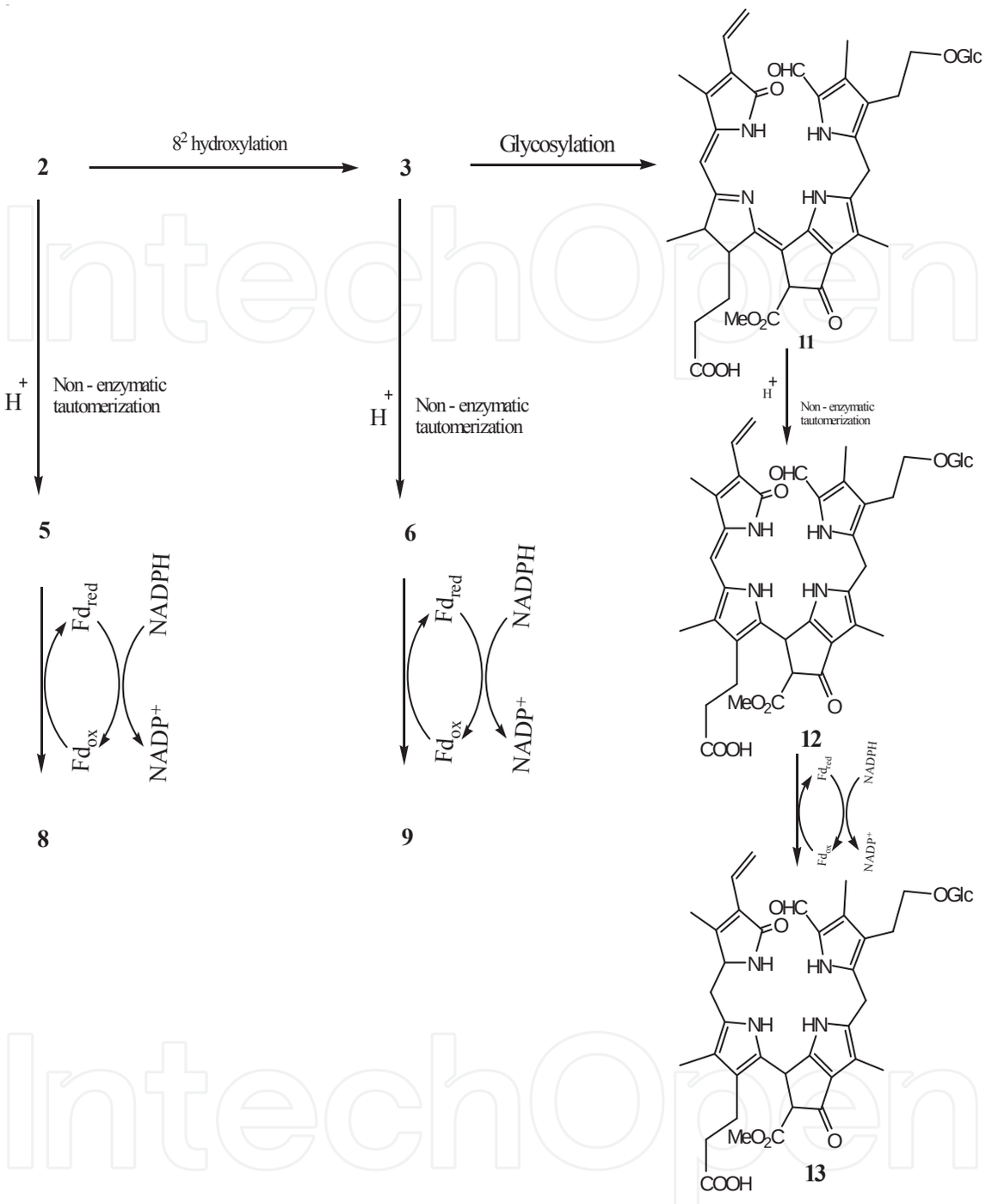

Figure 4. The chlorophyll biodegradation pathway in Solanaceae autumnal leaves, known up to now.

bridge. The reductase catalyzed reaction proceeds and the glycosylated chlorophyll biodegradation product 13 is formed.

The detection of other chlorophyll biodegradation products present in Solanaceae autumnal leaves will extend the chlorophyll biodegradation pathway, known up to now. The isolation of the sufficient quantity of the Solanaceae glycosylated chlorophyll biodegradation products

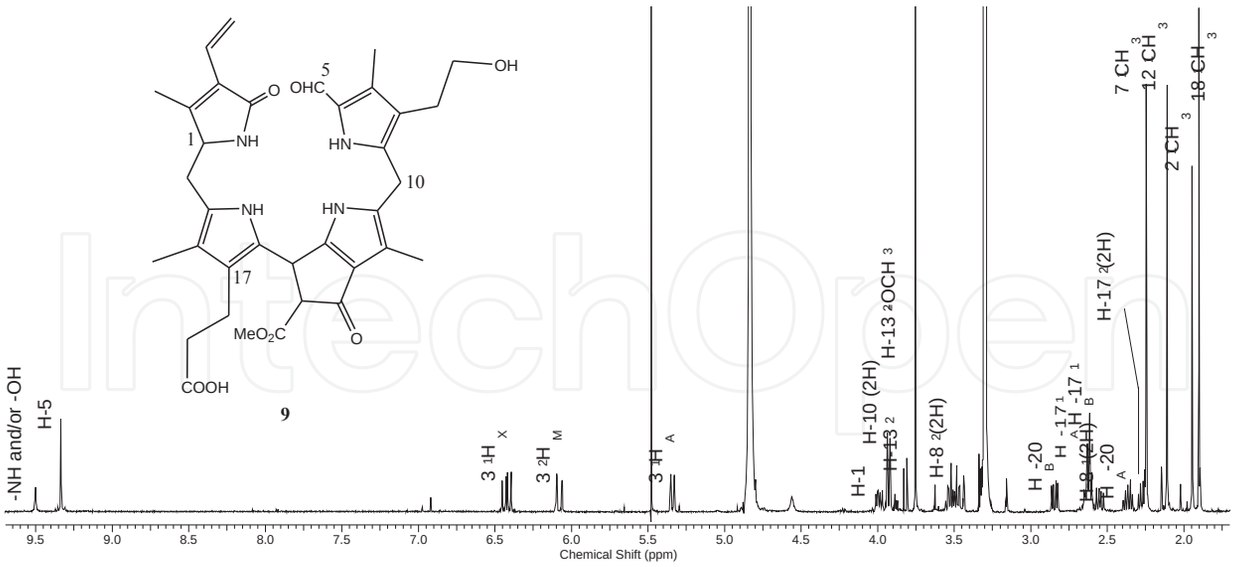

Figure 5. The proton spectrum of the compound 9.

will provide the information about the conformation of the sugar part and the information regarding the linkage between the aglycone and the sugar, such as, in the case of the anthocynins [22, 23, 24, 25].

5. Chlorophyll biodegradation in *Ginkgo biloba* autumnal leaves

Crude methanol extract of autumnal leaves' of *Ginkgo biloba*, Ginkgoaceae male plant were analyzed by LC-ESI-MS and LC/ESI-MS chromatograms and spectra obtained revealed the presence of the chlorophyll biodegradation products. Of hundreds of samples analyzed, only in one chromatogram obtained the traces the chlorophyll biodegradation product 9 with the molecular ion at *m*/*z* 645 for the molecular formula $C_{35}H_{40}N_4O_8$ was observed. Its proton NMR spectrum is depicted in Figure 5. Integration of the proton NMR spectrum revealed the presence of 33 protons. The signal of one proton on the heteroatom was still not exchanged with deuterium and was present in the low field region. The aldehyde H-5 proton signal was present in the low field region. Three low field *doublet of doublets* sets in the spectrum indicated the presence of an AMX spin-splitting pattern. The proton signal H-15 was overlapped with the HDO signal. Propionyl side chain H-17^1 protons came in a narrow δ range along with the methylene bridge H-20 protons. The H-17^2 protons, next to the electron withdrawing carboxyl group, had chemical shifts in the upfield region compared to H-17^1 protons. The most prominent peak in the proton spectrum was the signal assigned to the methoxycarbonyl group at the position 8^2. The methyl groups and other protons were assigned from the "1D difference" NOE spectra. In the COSY spectrum, the well resolved downfield 3^2 H_M vinyl proton was assigned to the geminal 3^2 H_A proton tracing further to the vicinal 3^1 H_X proton. This vinyl isolated spin system terminated at the 3^1 H_X proton.

All chromatograms obtained revealed the presence of three peaks, the UV detection at λ=312 nm. One peak had no Gaussian peak resolution (*Gb*-1), other two peaks coeluted with no separation to the baseline (*Gb*-2 and *Gb*-3) at the 25°C with gradient elution water (0.1% TFA): methanol on RP C_4 – analytical column (Figure 6). All peaks had the *m*/*z* 635. The ESIMS of the *Gb*-3 eluting at the 37.8 min. is depicted in Figure 7.

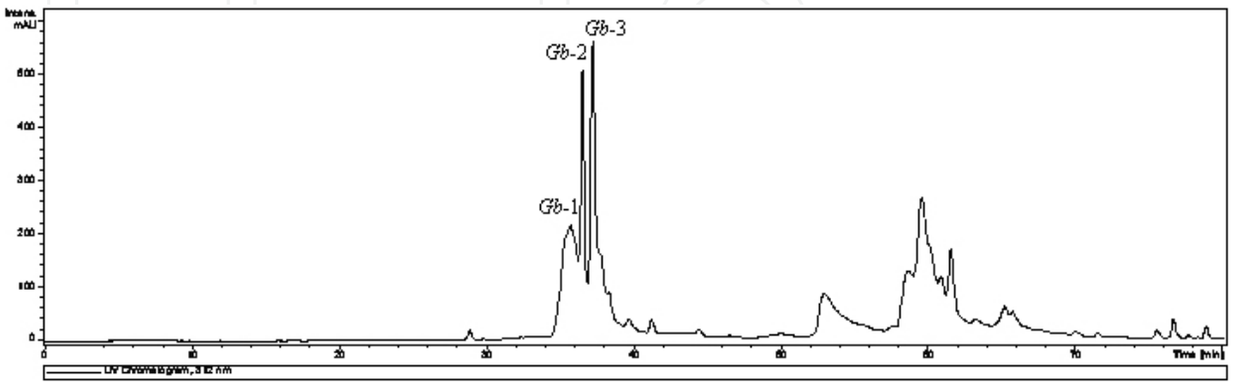

Figure 6. The chromatogram of *Gingko biloba* male methanol autumnal leaves' crude extract. The LC conditions: Column: Nucleosil 100-5 C_4 4x250 mm. The mobile phase: 90% v/v water (0.1% TFA):methanol to 0% v/v water (0.1%TFA):methanol in 80 minutes. Flow rate: 0.2 ml/min. UV detection at λ=312.

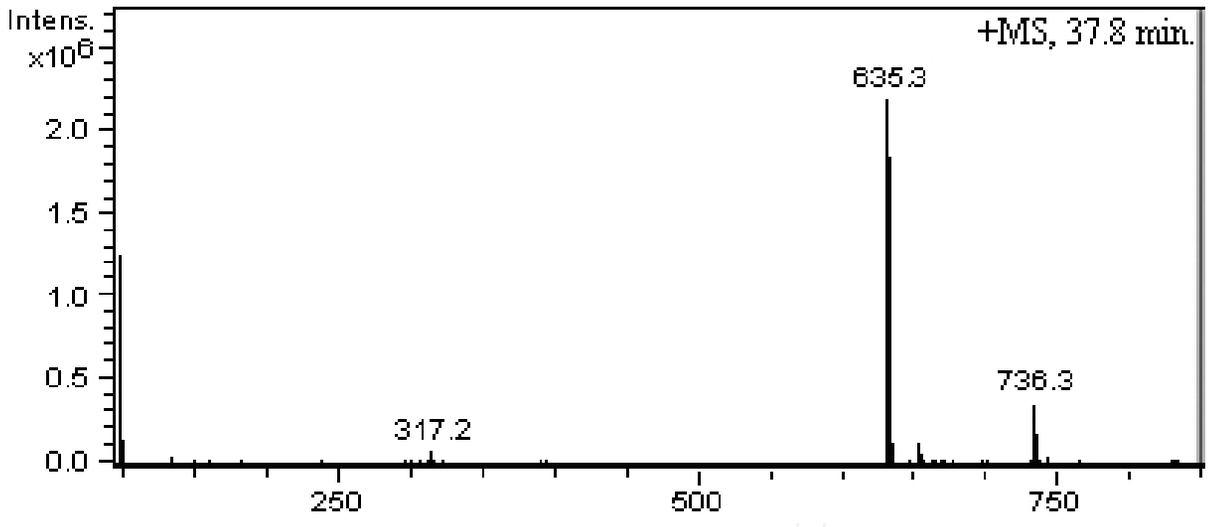

Figure 7. The ESIMS of the *Gb*-3 eluting at the 37.8 min.

The semi-preparative separation on one HPLC instrument on the semi-preparative RP-C_4 column with water (0.1% TFA): methanol solvent mixture gradient elution revealed the chromatogram (extracted at λ=312 nm) with complete peak distortion of *Ginkgo biloba* chlorophyll biodegradation products (Figure 8). The peak distortion was probably due to compounds' secondary equilibrium. It appears that the conversion rate of *Ginkgo biloba* compounds increased during the separation under the applied separation conditions. The

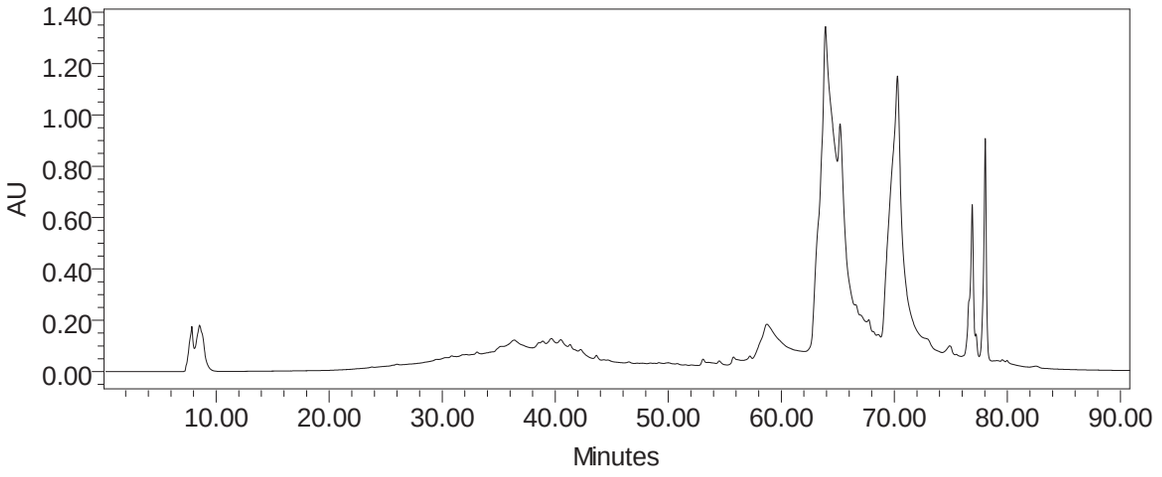

Figure 8. The chromatogram of *Ginkgo biloba* autumnal leaves, UV detection at λ=312 nm when the separation was done on one older model of the HPLC instrument

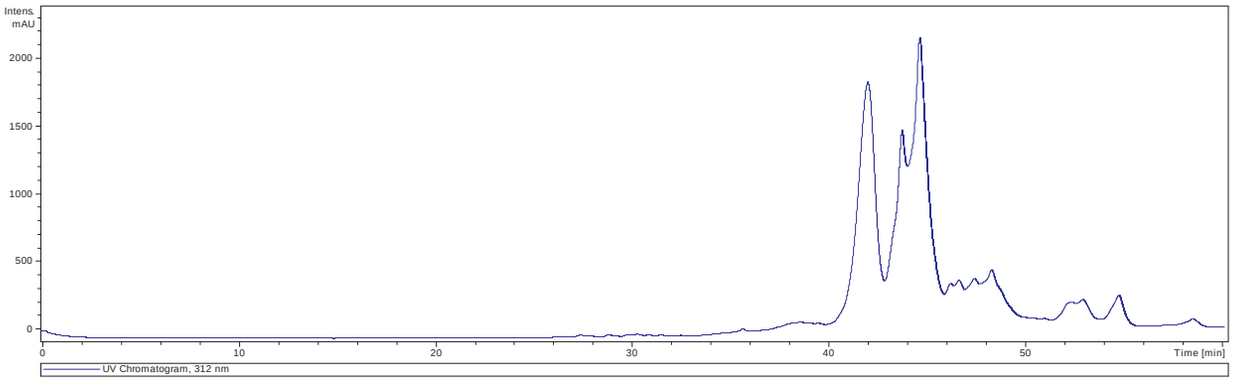

Figure 9. The chromatogram of *Ginkgo biloba* leaves' methanol crude extract. The LC conditions: Column: Nucleosil 120-7 C_4 10x250 mm. The mobile phase: 90% v/v water (acetate buffer): 10% v/v methanol to 0% v/v water (acetate buffer): 100% v/v methanol at 22°C in 90 minutes. Flow rate: 1.2 ml/min. UV detection at 312 nm.

peaks became smaller spreading over a long elution time (Figure 8). The UV spectrum of the broad peak from 40 to 42 min. revealed the presence of a chromophore with the absorption band of 317 nm. The *Ginkgo biloba* chlorophyll biodegradation products' peaks were broad and highly distorted.

The separation investigations continued on semi-preparative RP C_4 using the latest model of one LC instrument. The solvent mixture used was water (acetate buffer (pH 3.75)): methanol. The temperature was changed (Figure 9 and 10). At 30°C the separation between the peaks was observed (Figure 10). The isolation of *Ginkgo biloba* chlorophyll biodegradation products was done as depicted in Figure 10. Three collected fractions were evaporated under reduced pressure (t<40°C) and MS and NMR spectra were recorded.

http://dx.doi.org/10.5772/56155

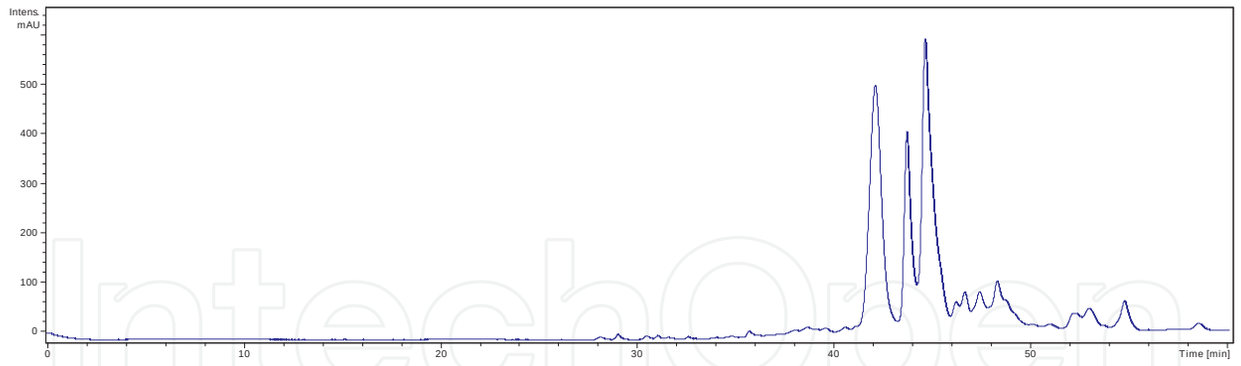

Figure 10. The chromatogram of *Ginkgo biloba* leaves' methanol crude extract. The LC conditions: Column: Nucleosil 120-7 C_4 10x250 mm. The mobile phase: 90% v/v water (acetate buffer): 10% v/v methanol to 0% v/v water (acetate buffer): 100% v/v methanol at 30^{0}C in 90 minutes. Flow rate: 1.2 ml/min. UV detection at 312 nm.

The compound eluting at 42 min. is assigned as the *Gb*-1, at the 44 min. as the *Gb*-2 and at the 45 min. as the *Gb*-3. The determination of *Ginkgo biloba* chlorophyll biodegradation products was done by mass spectrometry and NMR spectroscopy. The High Resolution Electron Spray Ionisation Mass Spectrometry (HRESIMS) of the *Gb*-1 showed a molecular ion at *m*/*z* 679.2350 for the molecular formula $C_{33}H_{37}N_4O_9Na_2$ $[M+2Na]^{2+}$, calculated *m* /*z* 679.2350, Δ 0.00 ppm. The other ion had *m*/*z* 657.2530 for the molecular formula $C_{33}H_{37}N_4O_9Na$ $[M+Na]^+$, calculated *m* /*z* 657.2531, Δ + 0.15 ppm. The formic acid was added to the sample and the HRESIMS was recorded. The mass spectrum obtained revealed the presence of *m*/*z* 679.2351 and *m*/*z* 657.2530. The *Gb*-2 had a molecular ion at *m*/*z* 679.2350 for the molecular formula $C_{33}H_{37}N_4O_9Na_2$ $[M+2Na]^{2+}$, calculated *m* /*z* 679.2750, Δ 0.00 ppm. The other molecular ion had *m*/*z* 701.2172 for the molecular formula $C_{33}H_{36}N_4O_9Na_3$ $[M+3Na]^{3+}$, calculated *m*/*z* 701.2170, Δ– 0.15 ppm. The addition of formic acid to the sample revealed the presence of the peaks *m*/*z* 657.2531, *m*/*z* 679.2347 and *m*/*z* 701.2166. For the *Gb*-3 compound, the Electron Spray Ionisation Mass Spectrometry (ESIMS) revealed the presence of three peaks, *m* /*z* 679.24, 701.22 and 723.20 when the sample was dissolved in methanol. The sample dissolved in methanol with formic acid revealed the presence of three peaks *m* /*z* 657.25, 679.24 and 701.22.

The proton NMR spectra were recorded. In the *Gb*-1 proton spectrum signals for the aldehyde proton were present, two well resolved *singlets* and one *pseudo triplet* (Figure 11). The *Gb*-2 and *Gb*-3 had the same signals in the low field (Figure 12 and 13).

The formyl group can have two conformations NO – *Z* (14) and NO – *E* (15) (Figure 14) [26, 27]. In all previously isolated *seco* – phytoporphyrins such conformational change has not been observed.

The vinyl group proton signals were of unresolved line shape (Figure 11, 12 and 13). The *doublet of doublets* were fairly broad at the room temperature. The vicinal proton of the vinyl group showed two superpositioned *doublets of doublets*. Similar to the proton spectrum of the chlorophyll biodegradation product 9, in the low field, three *doublet of doublets* sets in the proton spectrum indicated the presence of an AMX spin-splitting pattern (Figure 5, 11, 12 and 13). In the low field two sharp *singlets* were recorded (Figure 11). They were or impurities or the

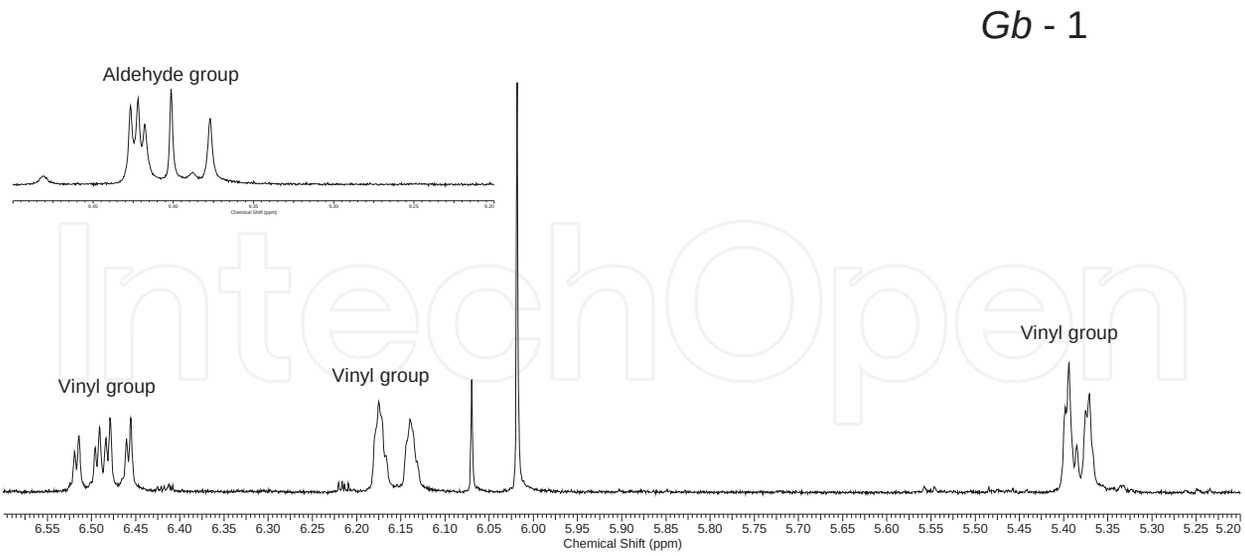

Figure 11. The enlarged proton spectrum of *Gb*-1 in the low field region

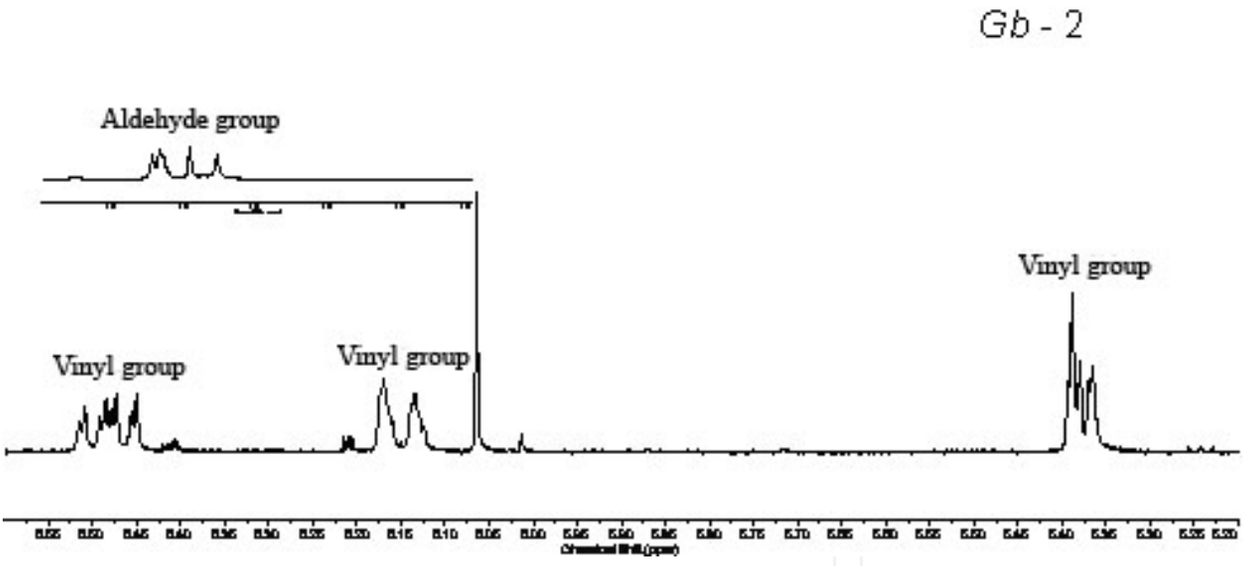

Figure 12. The enlarged proton spectrum of *Gb*-2 in the low field region

proton at the "western" methylene bridge. In the *Gb*-2 chlorophyll biodegradation product's proton spectrum in the vinyl region the proposed "western" methylene bridge proton gave one *singlet* (Figure 12). In the *Gb*-3 compound's low field proton spectrum only vinyl signals were recorded (Figure 13).

In all three *Gb* chlorophyll biodegradation products methoxy group of the five membered ring E was not present (Figure 15, 16 and 17).

http://dx.doi.org/10.5772/56155

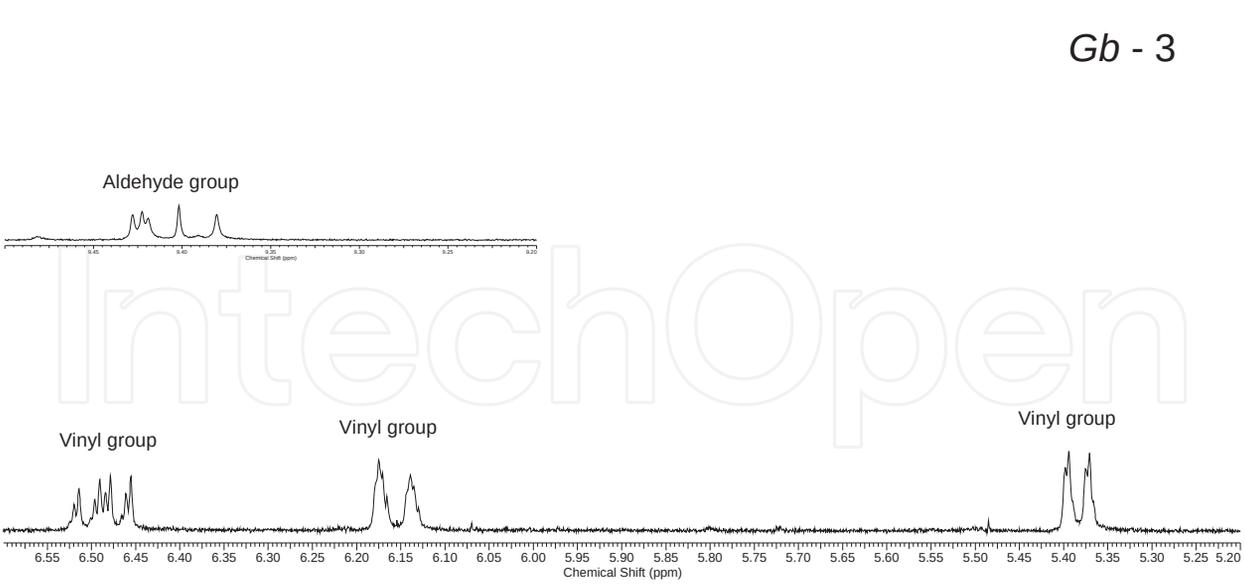

Figure 13. The enlarged proton spectrum of *Gb*-3 in the low field region

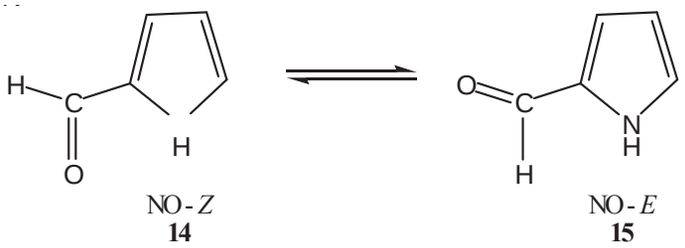

Figure 14. The conformational change of the pyrrole's aldehyde group

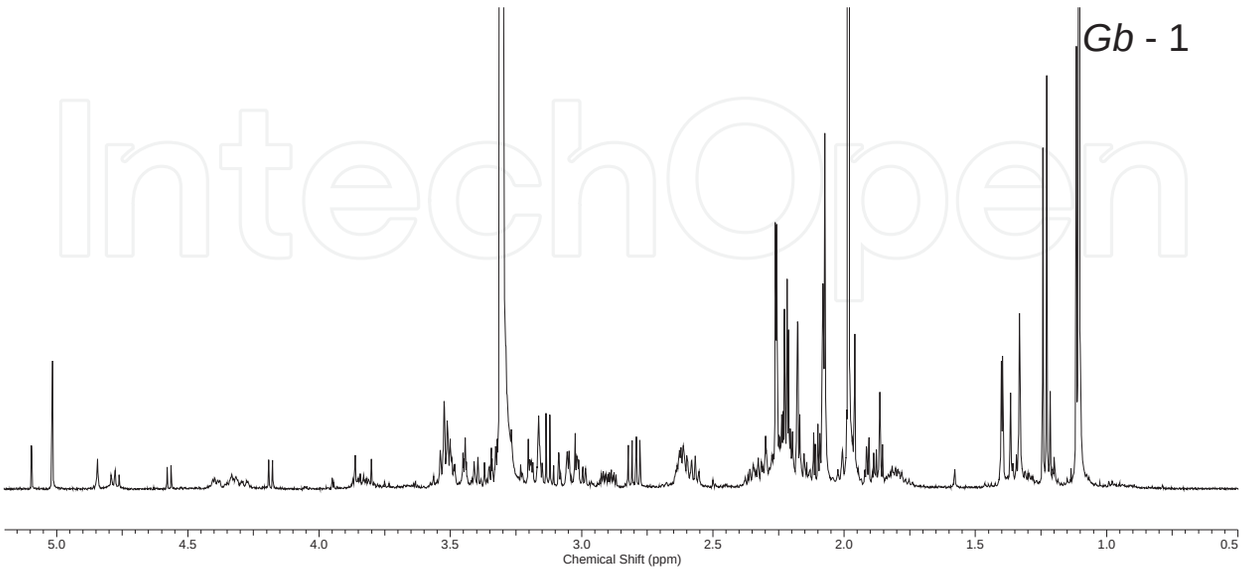

Figure 15. The proton spectrum of the *Gb*-1 in the high field region

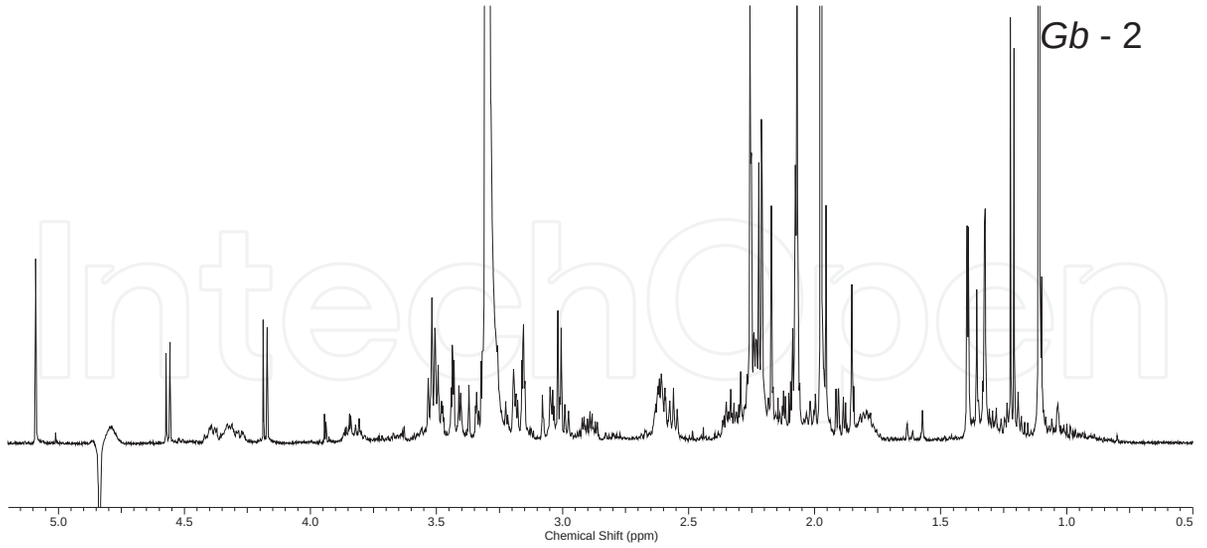

Figure 16. The proton spectrum of the *Gb*-2 in the high field region

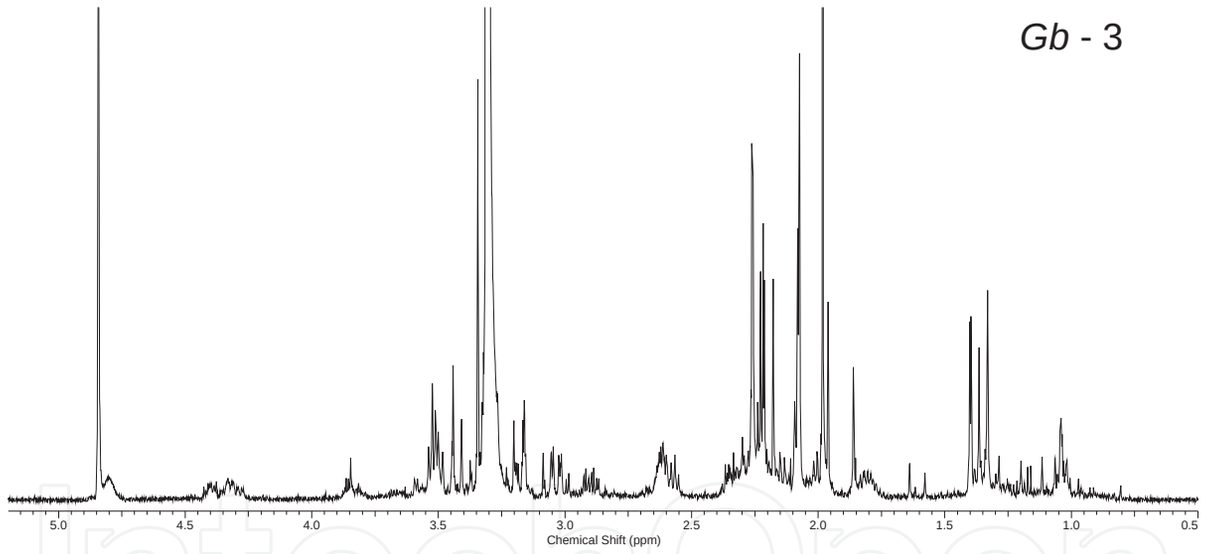

Figure 17. The proton spectrum of the *Gb*-3 in the high field region

The signals of the ethylene protons were found in all spectra recorded by the residual water peak. From the residual water peak to the high field region the presence of one *doublet* and one *doublet of doublets* was present. Those signals are, yet, not assigned. The methyl proton region is not similar to any previous chlorophyll biodegration products' high field region (Figure 15, 16 and 17). The chlorophyll biodegradation products found in *Ginkgo biloba* autumnal leaves are different from all previously isolated ones. The vinyl proton-proton connectivity in the COSY spectrum was easily observed (Figure 18). The *Gb*-3 COSY spectrum recorded was the same as the COSY spectrum of the chlorophyll biodegradation product 9 in the low field region. The establishment of other scalar coupled protons was not determined (Figure 19).

http://dx.doi.org/10.5772/56155

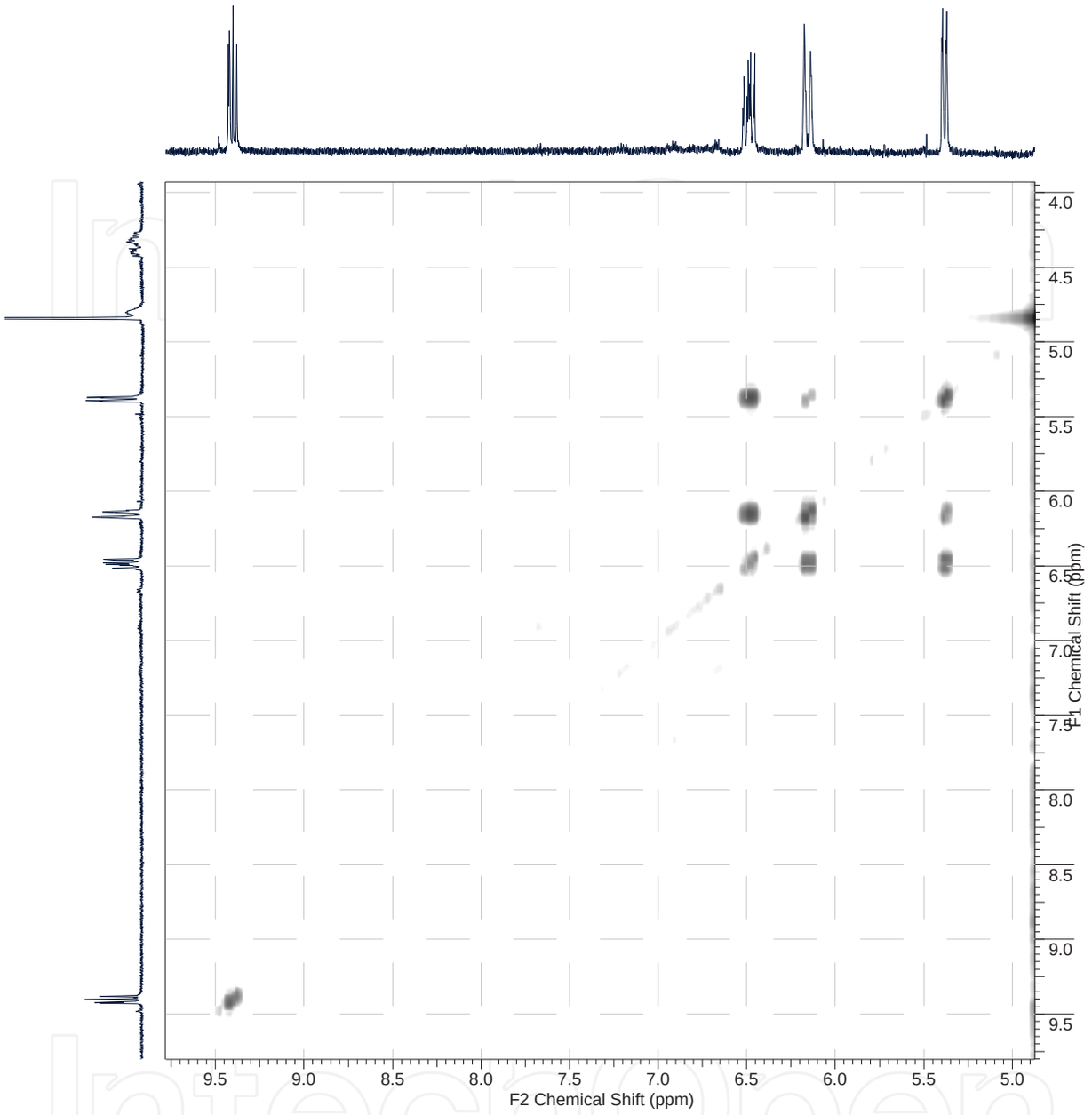

Figure 18. The COSY spectrum of the *Gb*-3 with the spectral expansion in the vinyl region

The dynamic NMR spectra were not recorded, yet, such as, they were done in case of the polycyclic quinones, substituted tetrahydropyrimidines, etc. [28, 29].

The *Ginkgo biloba* chlorophyll biodegradation products were, also, detected in the *Ginkgo biloba* female autumnal leaves' methanol crude extract (Figure 20).

The screening for the presence of the chlorophyll biodegradation products was done in ferns. Of dozens of ferns' autumnal leaves' methanol extracts analyzed only in *Athyrium filix femina*, Dryopteridaceae the *Ginkgo biloba* chlorophyll biodegradation products were detected (Figure 21). The cornifer plant – *Larix kaempferi*, Pinaceae autumnal leaves' methanol crude

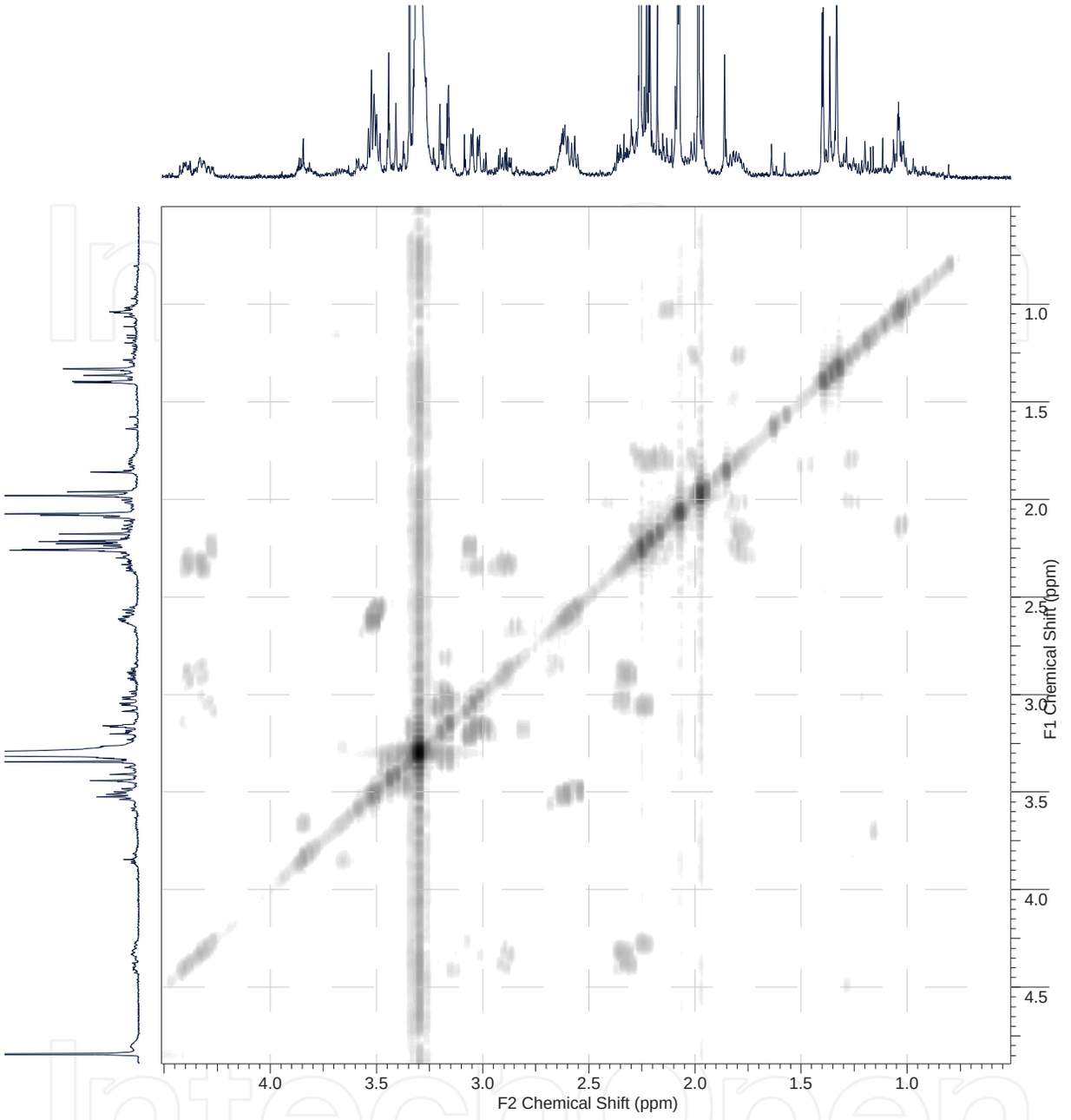

Figure 19. The spectral magnification of the *Gb*-3 COSY spectrum in the high field region

extract was analyzed and the *Ginkgo biloba* chlorophyll biodegradation products' were detected (Figure 21).

The chlorophyll biodegradation product 3 in Hamamelidaceae and Vitaceae autumnal leaves undergoes the oxidation of the aldehyde group at the C5 position forming the urobilinogenic chlorophyll biodegradation product 4.

In the Solanaceae autumnal leaves the chlorophyll biodegradation product 3 undergoes the glycosylation at the $C8^2$ position forming the glycosylated chlorophyll biodegradation product 11.

http://dx.doi.org/10.5772/56155

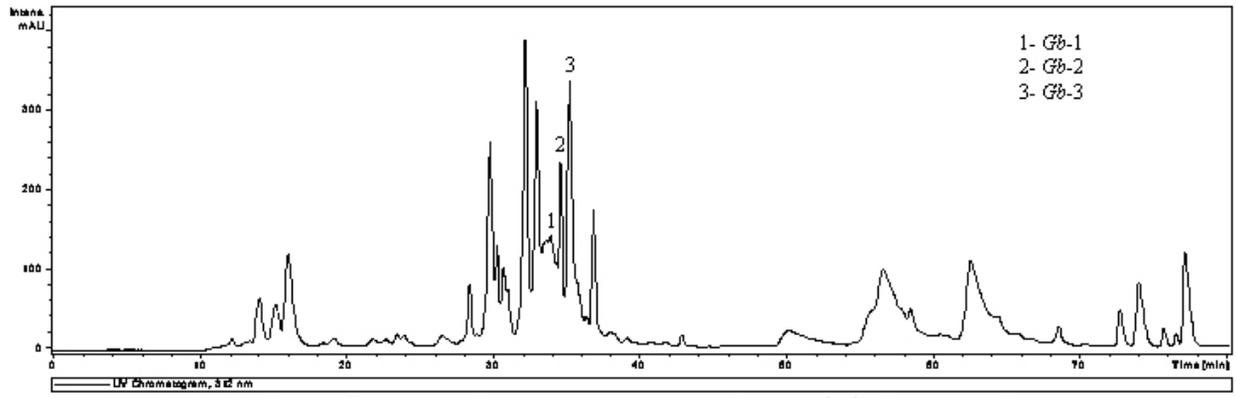

Figure 20. The chromatogram of the *Gingko biloba* female autumnal leaves' methanol crude extract. The LC conditions: Column: Nucleosil 100-5 C_4 4x250 mm. The mobile phase: 90% v/v water (0.1%TFA): methanol to 0% v/v water (0.1%TFA):methanol in 80 minutes. Flow rate: 0.2 ml/min. UV detection at λ=312.

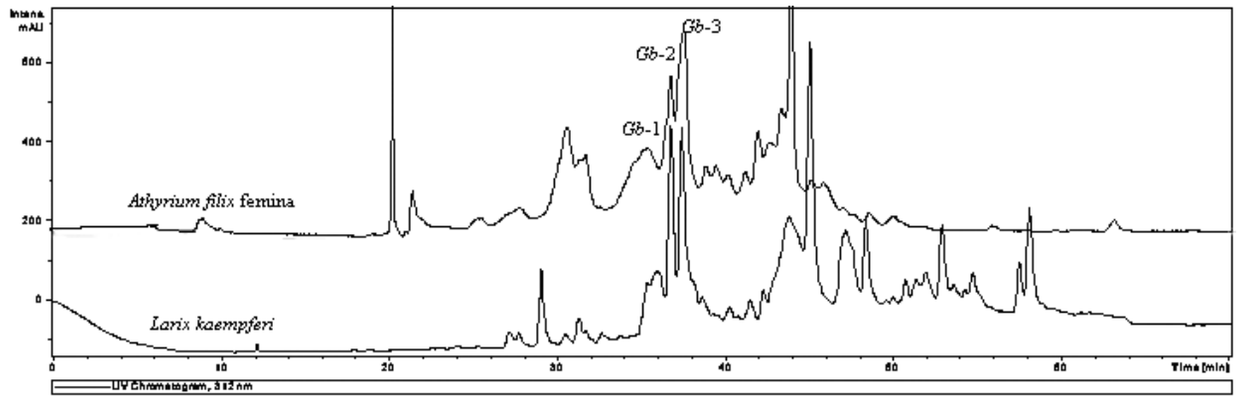

Figure 21. The chromatogram of *Larix kaempferi* and *Athyrium filix femina* autumnal leaves' methanol crude extract. The LC conditions: Column: Nucleosil 100-5 C_4 4x250 mm. The mobile phase: 90% v/v water (TFA): methanol to 0% v/v water (TFA):methanol in 70 minutes. Flow rate: 0.2 ml/min. UV detection at λ=312.

In the *Gingko biloba*, *Larix kaempferi* and *Athyrium filix femina* autumnal leaves the chlorophyll biodegradation product 3 undergoes the process that still has not been determined.

Further chlorophyll biodegradation products are colourless and were not identified, up to now.

6. The influence of ethylene on chlorophyll degradation

The ancient Egyptians used the ethylene to gas figs in order to stimulate ripening. The ancient Chinese used incense combustion to enhance the ripening of pears. In the 19th century, when the coal gas was used for street illumination, the trees in the vicinity of the street lamps showed extensive defoliation [30]. In 1901, Dimitry Nikolayevich Neljubov, observed that dark-grown pea seedlings growing in the laboratory exhibited symptoms that were later termed the triple response [31]. Dimitry Nikolayevich Neljubov identified ethylene, which was present in the

laboratory air from the coal gas, as the molecule causing the response [30]. Dimitry Nikolayevich Neljubov observation can be compared to Leonhard Euler's observation on seven bridges of Koenigsberg, which led to the formation of the Theory of Graphs [32]. Dimitry Nikolayevich Neljubov's observation led to the recognition of ethylene as a plant hormone [30]. In 1910, Herbert Henry Cousins reported that gas evaporation from stored oranges caused the premature ripening of bananas [33]. It was likely that the oranges used were infected with the fungus *Penicillium* which produces large amounts of ethylene. Herbert Henry Cousins showed that plants can produce their own ethylene [33]. In 1917, Doubt concluded that ethylene stimulates abscission [34]. In 1934, Gane reported that plants synthesize ethylene [35]. In 1935, Crocker proposed that ethylene is the plant hormone responsible for fruit ripening [36]. Ethylene, as well, has numerous effects on plant species and organs [30]. The peel of the citrus fruits requires ethylene to induce chlorophyll degradation [37]. The exposure of green leaves to ethylene can induce senescence only in leaves that have reached a defined age [38]. The biochemistry, genetics and physiology of ripening has been extensively studied in economically important fruit crops and the results obtained permitted the formation of the ethylene biosynthesis pathway, signaling and control of gene expression [39]. There is still much to be discovered about these processes at the biochemical and genetic levels.

Author details

Nina Djapic*

Address all correspondence to: djapic@tfzr.uns.ac.rs

Technical faculty "Mihajlo Pupin", University of Novi Sad, Zrenjanin, Serbia

References

[1] Brown, S. B, & Houghton, J. D. Hendry GAF. Chlorophylls. In: Scheer H. (ed.) CRC Press, Boca Raton, FL; (1991).

[2] Robinson, R. Richard Willstätter. (1872). Obituary Notices of Fellows of the Royal Society 1953; , 8(22), 609-634.

[3] Tswett, M. S. O novoy kategorii adsorbtsionnykh yavleny i o primenenii ikh k biokkhimicheskomu analizu. Trudy Varhavskago Obshchestva estevoispytatelei Otd Biol. (1903). , 14-20.

[4] Tswett, M. S. Physikalisch- chemische Studien ueber das Chlorophyll. Die Adsorptionen, Ber. Deutsch. Bot. Ges. (1906). , 24-316.

[5] Tswett, M. S. Adsorptionsanalyse und chromatographische Methode. Anwendung auf die Chemie des Chlorophylls, Ber. Deutsch. Bot. Ges. (1906). , 24-384.

[6] Tswett, M. S. in Chromophylls in Plant and Animal Worlds (1910). Warsaw University, Warsaw (in Russian).

[7] Stoll, A. in Ueber Chlorophyllase und die Chlorophyllide, Dissertation, Eidg. Technische Hochschule, Zuerich, (1912).

[8] Willstaetter, R, & Stoll, A. Untersuchungen uber Chlorophyll. XIX. Ueber die Chlorophyllide, Liebigs Ann. Chem. (1912). , 387-317.

[9] Ružicka, L. Biographical Memoirs of Fellows of the Royal Society (1972). , 18-566.

[10] KrasnovskyJr., AA. Chlorophyll isolation, structure and function: major landmarks of the early history of research in the Russion Empire and the Soviet Union. Photosynthesis Research(2003). , 76-389.

[11] Willows, R. D. Biosynthesis of chlorophylls from protoporphyrin IX, Nat. Prod. Rep. (2003). , 20-327.

[12] Ruediger, W. Biosynthesis of chlorophyll b and the chlorophyll cycle. Photosynthesis Research (2002). , 74-187.

[13] Shioi, Y, Watanabe, K, & Takamiya, K. Enzymatic conversion of Pheophorbide a to the precursor of Pyropheophorbide a in leaves of Chenopodium album, Plant and Cell Physiol. (1996). , 37-1143.

[14] Peoples, M. B, & Dalling, M. J. in Senescence and Aging in Plants (Eds.: L. D. Noodén, A. C. Leopold), Academic press, New York, San Diego, (1988). , 181.

[15] Djapic, N, & Pavlovic, M. Chlorophyll Catabolite from Parrotia Persica Autumnal Leaves. Rev. Chim. (Bucuresti) (2008). , 59(8), 878-882.

[16] Djapic, N, Pavlovic, M, Arsovski, S, & Vujic, G. Chlorophyl Biodegradation Product from Hamamelis virginiana Autumnal Leaves. Rev. Chim. (Bucuresti) (2009). , 60(4), 398-402.

[17] Djapic, N, Djuric, A, & Pavlovic, A. Chlorophyll biodegradation in Vitis vinifera var. Pinot noir autumnal leaves. Research Journal of Agricultural Sciences (2009). , 41(2), 256-260.

[18] Donoghue, N. A, Norris, D. B, & Trudgill, P. W. The purification and properties of cyclohexanone oxygenase from Nocardia globerula CL1 and Acinetobacter NCIB 9871, Eur. J. Biochem. (1976). , 63-175.

[19] Kelly, D. R. A proposal for the origin of stereoselectivity in enzime catalysed Baeyer-Villiger reactions, Tetrahedron: Asymmetry (1996). , 7-1149.

[20] Đapic, N. Behaviour of Fothergilla gardenii chlorophyll catabolite under acidic conditions. Kragujevac J. Sci. (2012). , 34-79.

[21] Djapic, N. private communication. (2012).

[22] Andersen, Ø. M, Aksnes, D. W, Nerdal, W, & Johansen, O-P. Structure elucidation of cyanidin-3-sambubioside and assignments of the ^{1}H and ^{13}C NMR resonances through two-dimensional shift-correlated NMR technique, Phytochemical Analysis, (1991). , 2(4), 175-183.

[23] Pedersen, A. T, Andersen, Ø. M, Aksnes, D. W, & Nerdal, W. Anomeric sugar configuration of anthocyanin O-pyranoside determined from heteronuclear one-bond coupling constants, Phytochemical Analysis (1995). , 6(6), 313-316.

[24] Andersen, Ø. M, Opheim, S, Aksnes, D. W, & Frøystein, N. Å. Structure of petanin, an acylated anthocyanin isolated from Solanum tuberosum using homo- and heteronuclear two-dimensional nuclear magnetic resonance techniques, Phytochemical Analysis (1991). , 2(5), 230-236.

[25] Nerdal, W, Pedersen, A. T, & Andersen, Ø. M. Two-dimensional nuclear Overhauser Enhancement NMR Experiments on Pelargonidin-glucopyranoside, an Anthocyanin of Low Molecular Mass. Acta Chemica Scandinavica, (1992). , 3.

[26] Farnier, M, Drakenberg, T, & Berger, S. Etude, par RMN, des conformations d'aldehydes α et β pyrroliques C-substitues. Stereospecificite des couplages lointains. Tetrahedron Letters, (1973). , 14(6), 429-432.

[27] Farnier, M, & Drakenberg, T. Nuclear Magnetic Resonance Conformational Studies of C-Substituted Pyrrolecarbaldehydes. Part 1. Substituent Effects on Aldehyde Conformations as shown by Long Range Coupling Constants. J. C. S. Perkin II (1975). , 4-333.

[28] Smirnov, A, Fulton, D. B, Andreotti, A, & Petrich, J. W. Exploring ground-state heterogeneity of hypericin and hypocrellin A and B: Dynamic and 2D ROESY NMR study. Journal of the American Chemical Society (1999). , 35(121), 7979-7988.

[29] Garcia, M. B, Grilli, S, Lunazzi, L, Mazzanti, A, & Orelli, L. R. Conformational Studies by Dynamic NMR. 84.[1] Structure, Conformation, and Stereodynamics of the Atropisomers of N-Aryl tetrahydropyrimidines. J. Org. Chem. (2001). , 66-6679.

[30] Taiz, L, & Zeiger, E. Plant physiology. 3rd edition. Sunderland: Sinauer Associates, Inc., MA. (2002).

[31] Neljubow, D. Ueber die horizentale Nutation der Stengel von Pisum sativum und einiger anderen Pflanzen. Beih Bot Zentralbl (1901). , 10-128.

[32] Alexanderson, G. L. About the cover: Euler and Koenigsberg's bridges: A historical view. Bulletin (New Series) of the American Mathematical Society (2006). , 43(4), 567-573.

[33] Cousins, H. H. Agricultural Experiments: Citrus. Annual Report of the Jamaican Department of Agriculture (1910). , 7-15.

[34] Doubt, S. L. The response of plants to illuminating gas. Botan. Gaz. (1917). , 63-209.

[35] Gane, R. Production of ethylene by some fruits. Nature (1934). , 134-1008.

[36] Crocker, W, Hitchcock, A. E, & Zimmerman, P. W. Similarities in the effects of ethylene and the plant auxins. Contributions of the Boyce Thompson Institute (1935). , 7-231.

[37] Purvis, A. C, & Barmore, C. R. Involvement of ethylene in chlorophyll degradation in peel of citrus fuits, Plant Physiol. (1981). , 68-854.

[38] Jing, H-C. Schippers JHM., Hille J., Dijkwel PP. Ethylene-induced leaf senescence depends on age-related changes and OLD genes in Arabidopsis. Journal of Experimental Botany (2005). , 56(421), 2915-2923.

[39] Chaves ALSCelso de Mello-Farias P. Ethylene and fruit ripening: From illumination gas to the control of gene expression, more than a century of discoveries. Genetics and Molecular Biology (2006). , 29(3), 508-515.

IntechOpen